Original Article

Landslides (2006) 3: 137–147
DOI: 10.1007/s10346-006-0035-2
Received: 16 February 2005
Accepted: 6 August 2005
Published online: 2 February 2006

H. B. Havenith · I. Torgoev · A. Meleshko · Y. Alioshin · A. Torgoev · G. Danneels

Landslides in the Mailuu-Suu Valley, Kyrgyzstan—Hazards and Impacts

Abstract Mailuu-Suu is a former uranium mining area in Kyrgyzstan (Central Asia) at the northern border of the Fergana Basin. This region is particularly prone to landslide hazards and, during the last 50 years, has experienced severe landslide disasters in the vicinity of numerous nuclear waste tailing dams. Due to its critical situation, the Mailuu-Suu region was and still is the target area for several risk assessment projects. This paper provides a brief review of previous studies, past landslide events and a discussion on possible future risk scenarios. Various aspects of landslide hazard and related impacts in the Mailuu-Suu Valley are analyzed in detail: landslide susceptibility, historical evolution of landslide activity, size-frequency relationship, river damming and flooding as well as impacts on inhabited areas and nuclear waste storage zones. The study was carried out with standard remote sensing tools for the processing of satellite imagery and the construction of digital elevation models (DEMs). The processed inputs were combined on a GIS platform with digital landslide distribution maps of 1962, 1977, and 2003, digitized geological and geographic maps, and information from landslide monitoring and geophysical investigation.

As a result, various types of landslide susceptibility maps based on conditional analysis (CA) are presented as well as predictions of future landslide activity and related damming potential and their possible impact on the population. For some risk scenarios, remediation and prevention measures are suggested.

Keywords Landslides · Hazard analysis · Socio-economic impacts · GIS · Kyrgyzstan

Introduction

Risk is the product of hazard and its socio-economic impact potential taking into account the value of the exposed objects and their vulnerability. In this equation, some terms are often misunderstood, such as hazard, which is often equated with susceptibility. In the case of landslides, Carrara et al. (1995) and Guzzetti et al. (1999) clearly outline the difference between hazard and susceptibility; the latter essentially describes the spatial distribution of the slope-failure potential whereas hazard also involves two other terms: the magnitude or intensity of a natural phenomenon and its temporal frequency or recurrence (Guzzetti et al. 1999).

This paper presents an analysis of hazards induced by numerous landslides in the Mailuu-Suu Valley (Kyrgyzstan). The link between hazards and the possible effects on the population is evaluated qualitatively without computing vulnerability and value of exposed objects; therefore, this study is not intended to be a risk analysis.

After a brief review of existing information about the environmental conditions, a landslide susceptibility (LS) analysis of the valley is shown. Among the various commonly used susceptibility mapping techniques based on neural networks (Lee et al. 2004; Fernández-Steeger 2002), fuzzy sets (Ercanoglu and Gokceoglu 2002) and multivariate models (Atkinson and Massari 1998) or physical (process-based) models (Vanacker et al. 2003; Khazai and Sitar 2000) we have chosen a statistical method, conditional analysis (CA), to assess the spatial landslide potential in the Mailuu-Suu Valley. This method has been successfully applied by Clerici et al. (2002) to assess LS in the Northern Apennines. This method has already been used for evaluating LS in the Suusamyr area located some 150 km north of the Mailuu-Suu Valley (Havenith et al. in press).

In addition to the LS, temporal and magnitude aspects of landslide hazard were studied on the basis of the size-frequency relationship, the historical evolution of landslide activity and landslide monitoring data. This allowed us to estimate future activity in terms of landslide recurrence within tens to a few hundred years.

Finally, several risk scenarios are presented and this is followed by a discussion on the likelihood of major events and their possible impacts on the population. In particular, we analyzed the potential of multiple simultaneous events and possible impacts from a so-called "Domino" effect. In a few of these cases, we had already reviewed proposed risk mitigation measures and suggested new ones, aiming to prevent future damage by delineating those zones most exposed to landslide hazards.

Study area

The Mailuu-Suu Valley (at 700–4,000 m altitude with 530 km² catchment area, semi-arid conditions) is located in the tectonically and seismically active Tien Shan Mountains. The Tien Shan is a Cenozoic orogenic belt in Central Asia with a basin and range structure caused by the post-collisional convergence of India with Asia. A major tectonic feature in the Tien Shan is the active Talas-Fergana fault crossing the mountain belt from NW to SE (Fig. 1).

Several strong earthquakes in the last century struck the Kyrgyz part of the Tien Shan (Fig. 1): the M = 8.2 Kemin earthquake in 1911, the M = 7.6 Chatkal earthquake in 1946 and the M_s = 7.3 Suusamyr earthquake in 1992. The area of Mailuu-Suu is characterized by a moderate to high seismic hazard (Abdrakhmatov et al. 2003). The last strong earthquake (Ms = 6.2) hit the region on May 15, 1992, and was located about 30 km SSE of the town of Mailuu-Suu (Fig. 1).

Another tectonically active zone, the Arslanbob area, is located in the north of the target region, the central Mailuu-Suu Valley, where the topography rises towards the Fergana Range (Fig. 1). The Fergana Range is partially built of Paleozoic rocks and bounded to the east by the Talas-Fergana fault. South of Mailuu-Suu, smooth hills formed by Tertiary sediments and Quaternary terraces dip towards the Fergana Basin (Fig. 1) which is the largest intramountain basin of the Tien Shan.

The central part of the Mailuu-Suu Valley is made of both Mesozoic and Tertiary rocks. Cretaceous (and locally Jurassic) rocks, mainly

Fig. 1 Shaded relief map of the Tien Shan Mountains (from NOAA digital elevation model) with location of Kyrgyzstan and neighboring countries, Talas-Fergana fault, Chatkal earthquake ($M_s = 7.6$, 1946), Suusamyr earthquake ($M_s = 7.3$, 1992), Kemin earthquake ($M_s = 8.2$, 1911) and $M_s = 6.2$ event in 1992, in the northern part of the Fergana Basin, 30 km south of Mailuu-Suu (indicated); A F: location of the Arslanbob fault in the northern Fergana Range

soft silt- and sandstones, form the core of open anticlines, such as the central anticline in Fig. 2, with steeper northern limbs. They are overlaid by alternating clay- and limestones of the Paleogene and Neogene. Several Quaternary terraces are located on both sides of the Mailuu-Suu River (Fig. 2).

Active slope failures were reported in the early 1950s, only a few years after the start of exploitation and processing of uranium deposits (mainly within Paleogene limestones) in 1946. Until the end of mining in 1968, the ecological situation in the valley became even more critical through the production of large amounts of nuclear waste, in part imported from Eastern Germany (Erzgebirge), Czechoslovakia (Yakhimov), Bulgaria (Bukhovo) and Tajikistan (Taboshar, Adrasman). At present, there are 23 tailings and 13 nuclear waste dumps with a total volume of about 3×10^6 m^3 of radioactive material along the banks of Mailuu-Suu River (Vandenhove et al. 2003). A major problem connected with the abandoned tailings is that erosion is degrading the protection measures, such as drainage systems and gravel covers.

Input data

The data used in this paper were collected over many years by different teams. Landslides have been counted since 1950 (after 1991, by geologists of the Ministry of Ecology and Emergency of the Kyrgyz Republic) using aerial photographs and field observations. Digital landslide maps are available for 1962, 1977, and 2003. The landslides include various kinds of coherent failures in rock (generally small rockslides) and earth slopes (debris and earth slides, slumps). Rock falls and debris flows were not mapped.

Detailed information about the nuclear waste storage was provided by the TACIS project *Remediation of Uranium Mining and Milling Tailing in Mailuu-Suu District* (Vandenhove et al. 2003). Previous studies including remote sensing analyses applied to the Mailuu-Suu area are described by Roessner et al. (2002).

In the frame of the NATO CLG project *Risk related to earthquakes, landslides and spreading of radioactive waste tailings in Mailuu-Suu, Kyrgyzstan* (2003–2004), we combined the existing information with remote sensing data. In addition, we digitized the landslide scarps as (buffered) lines to distinguish them from the main landslide body (the depositional area). The remote sensing data presented in this paper include the SRTM (Shuttle Radar Topographic Mission, 2000) DEM (~ 90 m resolution) and two ASTER images (northern part: 29/8/2001, southern part: 18/9/2002, 15–60 m resolution). From the

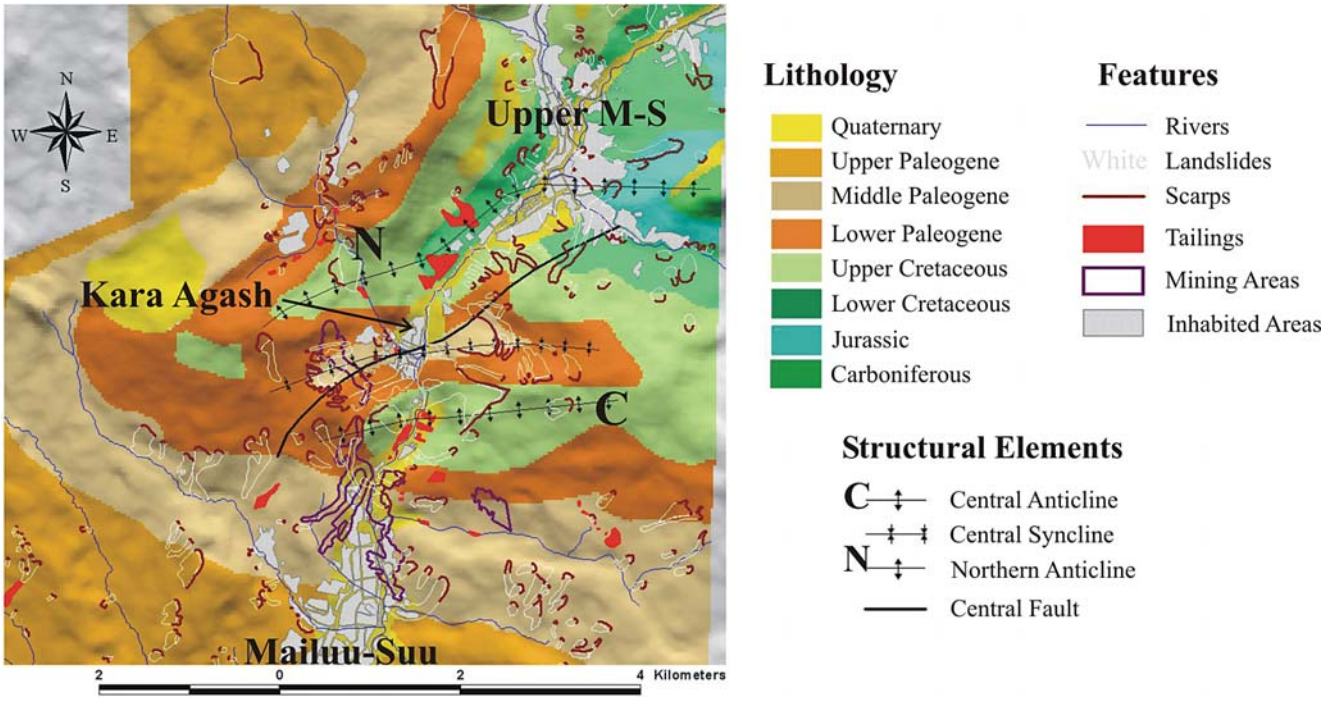

Fig. 2 Geological map of the central Mailuu-Suu Valley (Universal Transverse Mercator projection) with ASTER DEM hill-shading, location of rivers, landslides, tailings, mining areas, villages and town (Upper M-S : Upper town of Mailuu-Suu)

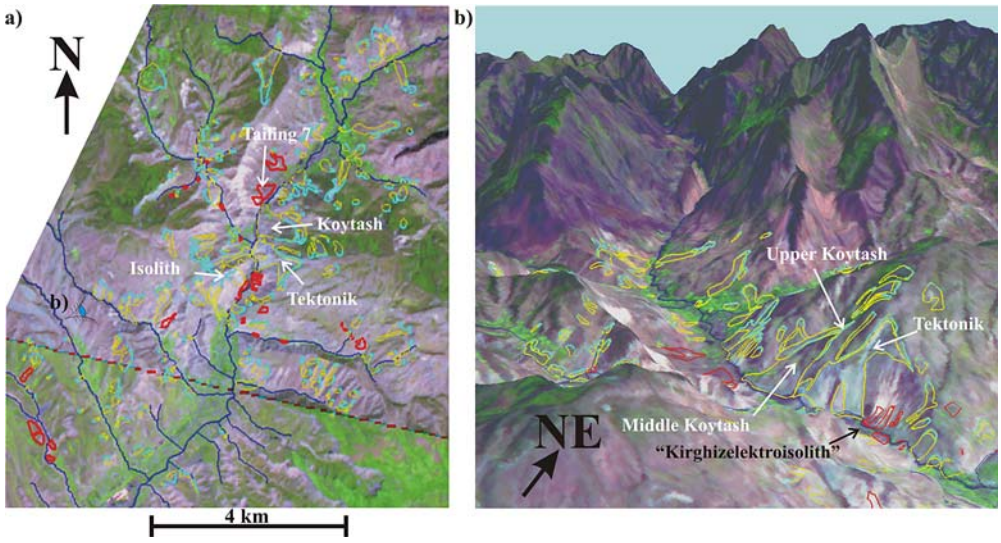

Fig. 3 Mosaic of ASTER images (limit marked by *dashed line*), 3-2-1 VNIR bands, with overlay of scarp (*light blue*), landslide body (*yellow*), river (*blue*) and tailing (*red*) outlines as vertical view with location of tailing no. 7, landslides Isolith, Tektonik and Koytash **a** and perspective view towards the central Mailuu-Suu Valley in the NE **b** with location of landslides Koytash and Tektonik as well as the factory Kirghizelektroisolith

ASTER images, DEMs were constructed with a resolution of 30 m using the method proposed by Al-Rousan et al. (1997). Several types of filters were applied to the models to remove artifacts: high-pass filter for filtering out low frequencies, segmentation for isolating holes and peaks, closing of holes, erosion of peaks, median filter, and dilation. This smoothed the elevation surface and has to be recognized when morphological aspects are discussed. The filtered DEMs extracted from the northern and southern ASTER images were merged to produce a mosaic. The images taken over a year were analyzed separately because they present different levels of reflectance (see northern and southern images in Fig. 3a).

Spectral information from the various bands of the ASTER images was extracted by principal component (PC) transformation. For the LS analysis, we used the three first principal component images extracted from the combination of the 3 VNIR (visible and near-infrared) and 6 SWIR (short-wave infrared) bands of the northern ASTER image covering most of the target area. Nadir and perspective views of the merged ASTER images (VNIR 3–2-1 bands) of the central Mailuu-Suu Valley are shown in Fig. 3a, b.

Landslide activity

The onset of major slope destabilization in the Mailuu-Suu Valley is connected with the start of mining in 1946. It should be mentioned, however, that 24 ancient landslides already existed; they are not well documented—literature about landslide activity before 1946 is scarce—but show that mining is not the only trigger of slope instability in the valley.

Twenty-nine new landslides were observed in 1950; they occupied 1% of the slopes along the middle Mailuu-Suu Valley. Large slope movements with impacts on the local population started in 1953–54 at the foot of the Isolith, Koytash and Tektonik landslides (located in Fig. 3). Slumping of Isolith caused significant damage in the "Kyrgyzelektroisolith" Plant (Fig. 3b). Movement of these landslides continued in the 1960s with the development of cracks, mudflows, and minor rock falls. Mining stopped in 1968, but landslide activity continued. The biggest disaster occurred on July 4, 1992, when 1.5×10^6 m^3 of rock material collapsed and formed landslide Tektonik (Fig. 4a). It buried tailing no. 17 (no more visible), dammed Mailuu-Suu River and partly destroyed the aforementioned "Kyrgyzelectroisolith" Plant (Vandenhove et al. 2003). The landslide dam (15 m high and more than 100 m wide) was eroded by overflow after a few days. Since that time, Tektonik has dammed the Mailuu-Suu River several times (in 1994, 2002, and 2005), inducing major up- and downstream flooding.

Tektonik is a complex landslide with (multi-rotational) slumping in the upper part and recent formation of a new scarp 120 m behind the main head-scarp (Fig. 4). In the lower part it became an earth slide where, seasonally, debris flows develop on its surface. The 1992 Tektonik event occurred 7 weeks after an $M_s = 6.2$ earthquake (May 15, 1992) located 30–40 km SSE of the site (Fig. 1). Nothing is documented about the slope before the earthquake and during the following 7 weeks (dry period, after snowmelt and rain in spring). Therefore, it is difficult to determine which contributed more to cause the mass movement, mining or the earthquake. Possibly, Tektonik is the product of several actions: existing creep or lowered factor of safety caused by the mining was accentuated by the seismic ground motions (peak ground acceleration of the order of 0.1–0.15 g without considering amplification effects) and turned into a rapid mass movement due to particular ground-water conditions (with interaction of meteorological factors).

According to Torgoev et al. (2002), the link between the mining and landslides in the Mailuu-Suu Valley can be explained by the fact that the rock massif was weakened by the extraction works. When the mines were abandoned in 1968, many slope failures were induced by collapse of underground galleries located at a depth of 30–40 m (at some places, subsidence affects also the surface).

Another mechanism that may explain the increase in slope instability is a possible rise of ground water in the abandoned mines. Slopes fail preferentially close to the Central fault, and this may be due to enhanced ground-water flow along the fault zone. This fault zone crosses the principal mining zone and could contribute to high ground water in these areas.

Development of landslides in the Mailuu-Suu Valley in connection with mining can be considered as similar to the triggering of landslides by an earthquake: mining may have induced additional fracturing and weakening of the soft and hard rocks and triggered minor slope failures—similar to the co-seismic effects of earthquakes on slopes; the collapse of galleries after the end of mining could be compared with the impacts of after-shocks; modified groundwater conditions are observed both after abandonment of mines and after seismic events. The aim of this comparison is to show that landslide activity in

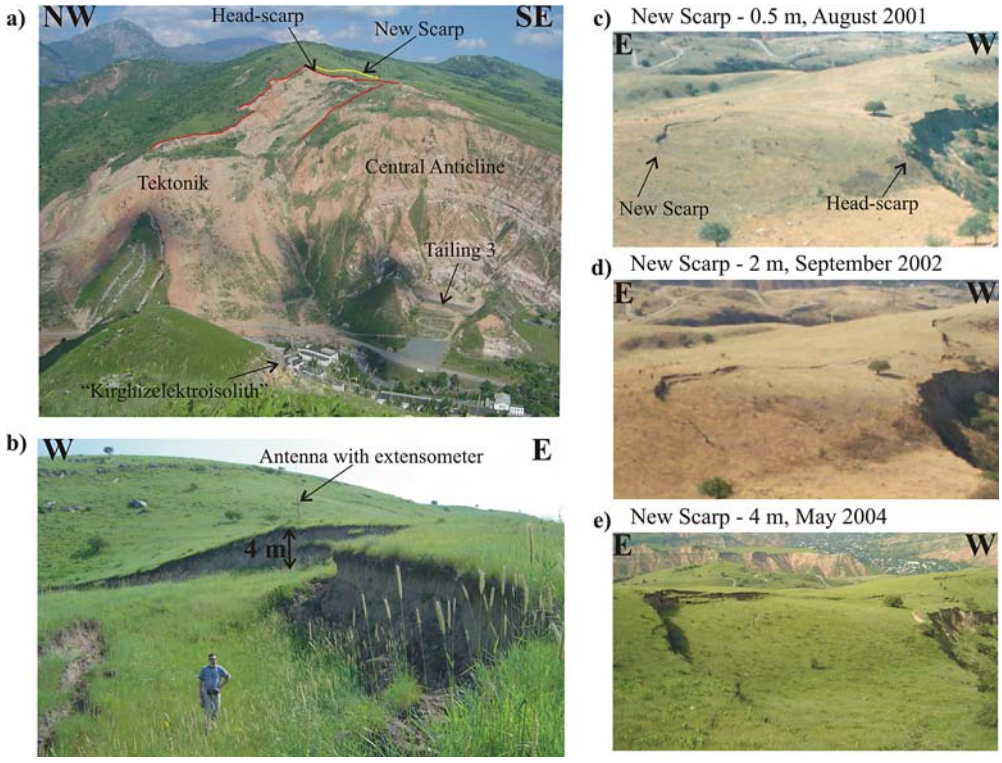

Fig. 4 **a** Landslide Tektonik (view towards NE), May 2004; b 4-m-high new scarp with monitoring antenna; **c–e** evolution of the new scarp from August 2001 till May 2004, photos c and d are taken from Vandenhove et al. (2003)

the Mailuu-Suu Valley is neither spatially nor temporarily stationary (landslides are not being triggered more-or-less regularly over time).

Medium- to long-term changes can be inferred from landslide occurrences since 1950 (Fig. 5). Landslides were classified into four main groups according to their state of activity: incipient landslides (initiating slope failure), landslides with little movement (mostly slumping), landslides with ongoing movement (slumping turning into sliding), and stabilizing landslides (post-sliding creep). During the survey period, stabilizing landslides (2 in Fig. 5) were the most numerous ones, followed by landslides with repeated movements (3 in Fig. 5). The number of all types of landslides is increasing with time, except for incipient failures which have become less numerous over the last 10 years. An increase in landslide activity was observed during, or just after, years with abundant precipitation, such as in 1954, 1969, 1978, 1994, 2003 (see Fig. 5). The dependence of landslide movement on meteorological factors is confirmed by recent detailed measurements shown at the end of this section.

The increasing number of landslides also implied an increasing total area of failed slopes, about 0.5 km² (~ 1% of all slopes in the Mailuu-Suu Valley) in 1950, 1.2 km² (~ 2.5%) in 1962, 2.4 km² (~ 5%) in 1977 and 4.7 km² (~ 10%) in 2003. Over the period during and after mining, increases in the number and area of all landslides are roughly linear. These trends could be used for predicting the future evolution of landslide activity: by 2100, the total landslide area could be about 16–17 km² (30% of the total area). The reliability of such a forecast is discussed at the end of the paper when other elements have been analyzed. Further, we need to consider the dependence of landslide activity on storms, wet seasons, and earthquakes, which may strongly affect the future evolution.

In order to further characterize the landslide activity, size–frequency relationships were computed for the three available landslide data sets of 1962, 1977, and 2003. These are compared in Fig. 6 with statistics of a landslide-rockslide inventory (446 records) for the Suusamyr region recently analyzed by Havenith et al. (in press). According to the method of Malamud et al. (2004), the size–frequency relationship of these data sets was analyzed in terms of the frequency density function (f) of landslide areas (A_L Eq. (1)):

$$f(A_L) = \frac{\delta N_L}{\delta A_L} \tag{1}$$

where δN_L is the number of landslides with areas between A_L and $A_L + \delta A_L$.

This function follows a power-law, with decreasing frequency density for larger areas. This trend breaks down for small areas and shows a so-called roll-over (with decreasing frequency density for very small landslide areas). Such roll-overs are often explained as incompleteness of the data set. Malamud et al. (2004), however, consider their landslide inventories as complete well below the roll-over, and hence regard the latter as "real", but do not explain its origin. From Fig. 6 it can be seen that the roll-over occurs for smaller landslide areas in the case of the Mailuu-Suu landslide data sets compared with the Suusamyr landslide-rockslide data set (Fig. 6). For the latter, the maximum frequency density is computed for an area of about 7,500 m² whereas it is about 2,500 m² for the Mailuu-Suu landslide data set. Malamud et al. (2004) noticed that all their analyzed landslide data sets reveal a maximum probability density for 400 to 500 m. Our data sets appear to be incomplete for landslides smaller than ~ 10,000 m² in the case of the Mailuu-Suu data sets and smaller than ~ 100,000 m² in the case of the Suusamyr data set.

Power-law trends were fitted to the data larger than these areas. For the Mailuu-Suu landslides of 1962 and 1977, the exponents are 2.23 and 2.43, similar to values found by Stark and Hovius (2001) and Malamud et al. (2004) for various types of landside distributions. The power-law exponents for the 2003 Mailuu-Suu and Suusamyr records are 1.9 and 1.94, respectively, significantly lower than values obtained

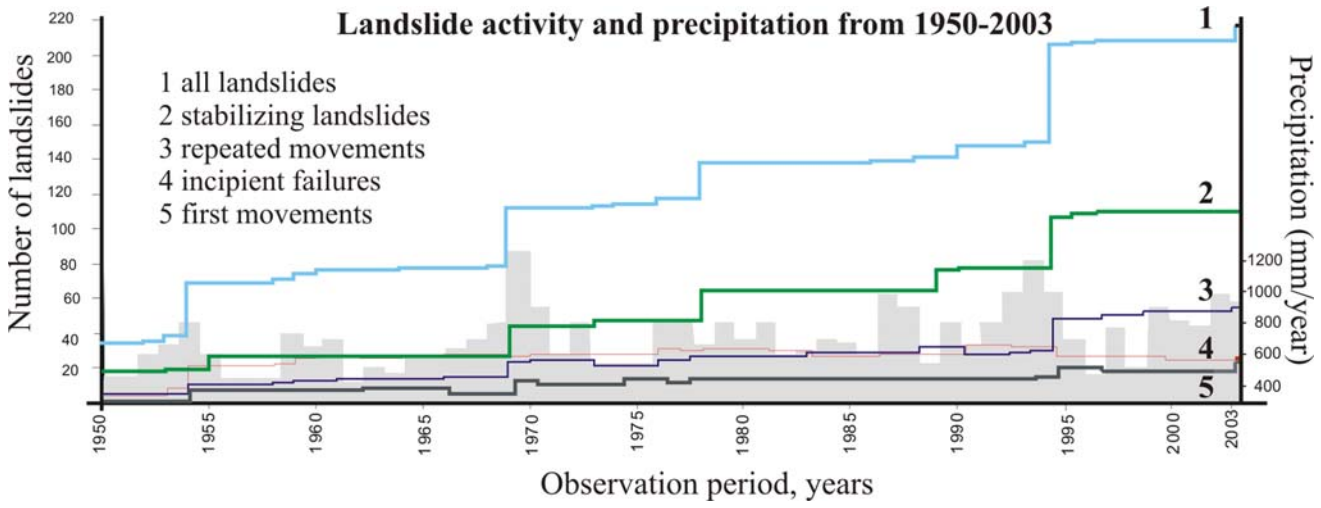

Fig. 5 Landslide activity (number of landslides with various types of activity) versus precipitation (*grey*) from 1950–2003

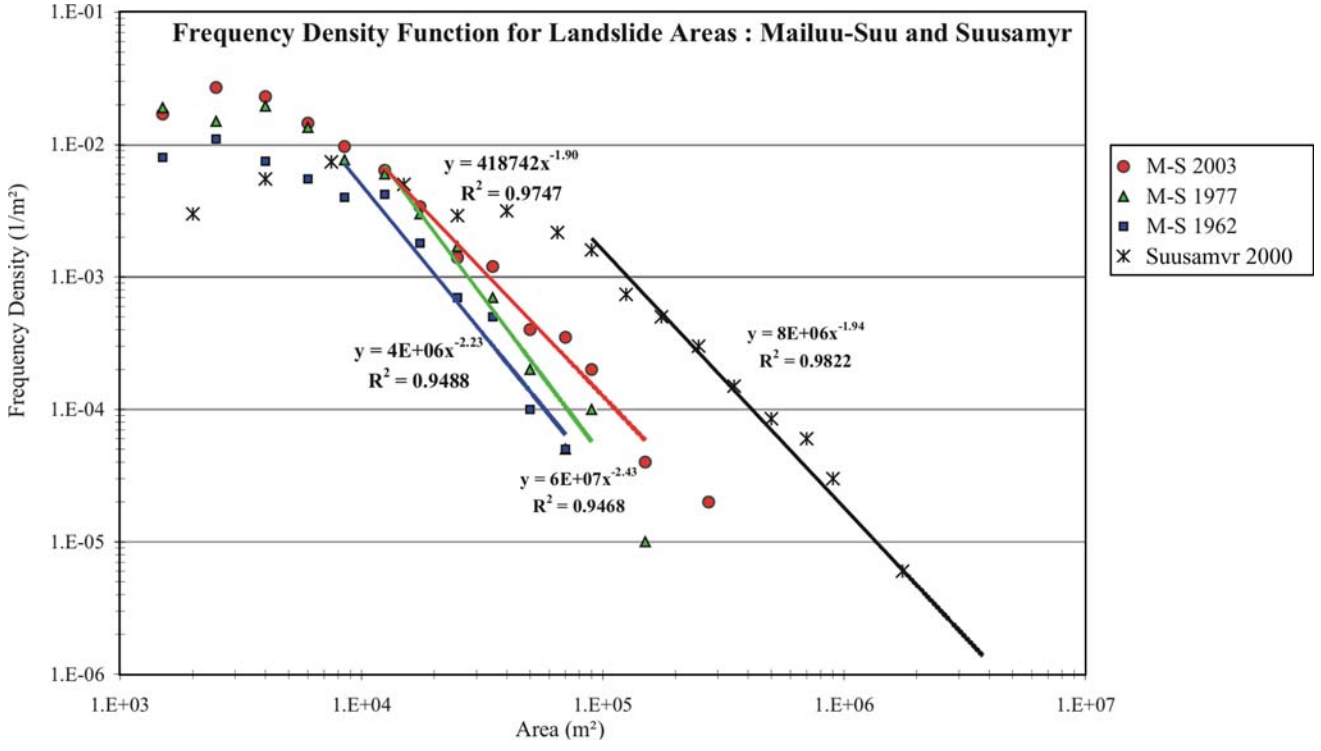

Fig. 6 Frequency-density function for landslide areas in the Mailuu-Suu Valley in 1962 (78 events), 1977 (117 events) and 2003 (220 events) compared with the frequency-density distribution of landslides and rockslides in the Suusamyr region (446 events)

for landslide inventories analyzed by the cited researchers. These trends are, however, consistent for records of large landslides, which can be considered complete and reliable. In the case of the Suusamyr records, no particular reason was found to explain the low exponent. The particular power-law behavior of the 2003 Mailuu-Suu landslide distribution could be explained by the formation of large landslides by coalescing smaller landslides (or growth of smaller landslides) so that the number of smaller landslides has been reduced with time (note also the slightly decreasing number of incipient landslides). A prominent example of a growing landslide is Tektonik as shown in Fig. 4. Coalescing slope failures produced large earth slides and flows in the West of Mailuu-Suu (see double scarps just below the name "Isolith" in Fig. 3a). This evolution is likely to continue.

Failure mechanisms and landslide growth are also being analyzed in more detail. Slopes at risk of failure have been monitored since 1996 and their structures investigated with geophysical and geotechnical methods (surface extensometers and borehole measurements). Displacement data are either manually collected or transmitted by radio (e.g., antenna on Tektonik shown in Fig. 4b) to a central collection point (formerly, inside the Kirghizelektroisolith factory—now under

reconstruction). This system connects to a warning system for emergency response action if rapid movements occur (40 mm/24 h)—an alarm is triggered and a local evacuation may be started.

Correlations between slope movements and climatic conditions, i.e., snow cover and precipitation, as well as seismic activity are shown in Fig. 7 for the Middle Koytash and Upper Koytash (location in Fig. 3b). Similar records exist for several other landslides, such as Tektonik and Isolith. From these data, it can be inferred that the landslides reactivate each year, mainly at the end of spring and beginning of summer, due to high groundwater level after snowmelt and the spring rains. Some reactivations can also be attributed to seismic shocks such as the movement of Upper Koytash after a relatively shallow (depth $\sim$22 km) $M_s = 5.9$ earthquake that occurred on 9/1/1997 in the Osh district at an epicentral distance of $\sim$150 km from the site (note the very low acceleration expected for the site <0.05 g if no amplification is taken into account).

The Koytash landslide is moving slowly, averaging less than 40 cm per year in the upper part and about 60 cm per year in the middle part. Some landslides, however, move faster, such as for example the Isolith landslide, which averages about 1.5 m per year. The largest daily displacement (60 cm in 2 days) was recorded on Upper Koytash after the $M_s = 5.9$ earthquake in January 1997.

Landslide susceptibility

A critical question raised above concerns the potential for future landslides. Therefore, LS was assessed for the Mailuu-Suu Valley using the Spatial Analysis extension of the Arcview 3.2 software. All available information was used in grid (raster) format: the 30-m ASTER DEM, the 15-m principal component (PC) images and the geological map. Vectors, such as scarps, landslide bodies, and fault outlines (only the Central fault shown in Fig. 2 was included) were transformed into raster format by computing grids of distances from each feature. In the case of the scarps, the values of pixels within 30 m from the scarp outlines were set to 1, the others to 0 (i.e., a 30-m external and internal buffer). The entire detachment area was not used, in order to determine the conditions, which lead to rupture at the surface (i.e., visible at the surface to be used as indicator for future scarp formation). For landslide deposits, the area within landslide polygons as well as the surrounding 30-m buffer was used. For the Central fault zone, the whole distance-to-fault map was reclassified into five units (five classes between 0 and 7,500 m).

The topographic information (30-m ASTER DEM) was processed in terms of slope, aspect, and tangential curvature. Smoothing of the DEM described earlier affected calculation of the morphological factors. Calculated slope angle and curvature are especially likely to be less than in reality. Hence, they should be considered as relative indices rather than as absolute values.

The role of the various morphological factors in determining LS is only briefly discussed in this section. For more detailed discussion we refer the reader to the works of Ayalew et al. (2004), Gritzner et al. (2001) and Lee et al. (2004) and to a previous study (Havenith et al. in press). The susceptibility analysis is based on the following factors: slope, aspect, curvature, geology and fault distance maps as well as the 3 PC image-grids.

Landslide factor analysis

A preliminary factor analysis was carried out to roughly define the influence of each factor on landslide body or scarp location. This first approach uses the correlation between landslide body (scarp) distribution and pixel values of the various factors. It computed the densities scaled for the specific map extent of landslide masses, *Lm*, (or scarps, *Sc*) within a factor class using Eq. (2). This allowed us to define the type of slope most prone to scarp formation or landslide mass deposition.

Scarps preferentially develop (have highest density) on slopes of 12–18°, oriented towards the NE or W, characterized by a slight convex (tangential) curvature and located in lower Paleogene or lower Cretaceous rocks close to the Central fault. Landslide bodies are located on similar types of slopes, but those characterized by a slight concave curvature. Jurassic rocks are also landslide prone, but cover only a very small area in the region, hence, their presence does significantly influence LS over the entire area.

$$Sc(Lm) = \frac{buffer - class - counts}{class - counts} \bullet \frac{map - counts}{buffer - counts} \qquad (2)$$

where *Sc (Lm)* is the map-scaled scarp (landslide mass) density, *buffer-class-counts* the number of pixels of the same class within all scarp (landslide mass) buffers, *class-counts* the number of all pixels in the same class, *map-counts* the total number of pixels within the map and *buffer-counts* the number of pixels within all scarp (landslide mass) buffers.

It may seem surprising that failures develop on relatively gentle slopes; however, the DEMs were smoothed and hence computed slope angles (and also curvatures) are smaller than the real ones. Also, high slopes generally characterize hard rock massifs, which are less prone to (here investigated) slope instability.

Correlations were also made with distance from mines, rivers, and roads; they generally show a spatial proximity between slope failures and these features. In particular, the distance from mines seems to have an influence on LS while the influence of the other factors on slope stability could not be well outlined. For the final LS mapping we did, however, not include the anthropic effect.

Conditional analysis

The main part of the LS analysis is based on the conditional analysis. It consists of subdividing the entire area into pixels characterized by a specific combination of factors (Carrara et al. 1995), or conditions – termed unique condition units (UCUs). Thus, each pixel of the resulting digital map is characterized by a new index. In order to evaluate the landslide susceptibility of the UCU, we computed the map-scaled scarp (landslide mass) densities for each UCU according to Eq. (2) where *class* means UCU, a combination of factor classes ("natural breaks" used as reclassification).

Several studies (e.g., Carrara et al. 1995) suggest applying neighborhood majority filtering after each new combination of two factor grids. This approach was not applied here because it significantly reduces the efficiency of the method. A major disadvantage of not including filtering during computation is that the number of UCU produced by combinations of many factor classes can be very large and cause computation problems.

The outcomes of the LS analysis were analyzed with regard to ten (out of 20) different factor-combinations made over three different map extents (GEOLOGY map, northern ASTER image and ASTER mosaic). The results are presented in Table 1 in terms of maximum map-scaled densities and the respective counts (number of pixels of the UCU), and in terms of predictive power (PP) of the resulting LS map. We defined the predictive power as:

$$PP = \frac{\text{average of the 10\% of the most susceptible UCU}}{\text{average of the 90\% of the least susceptible UCU}} \qquad (3)$$

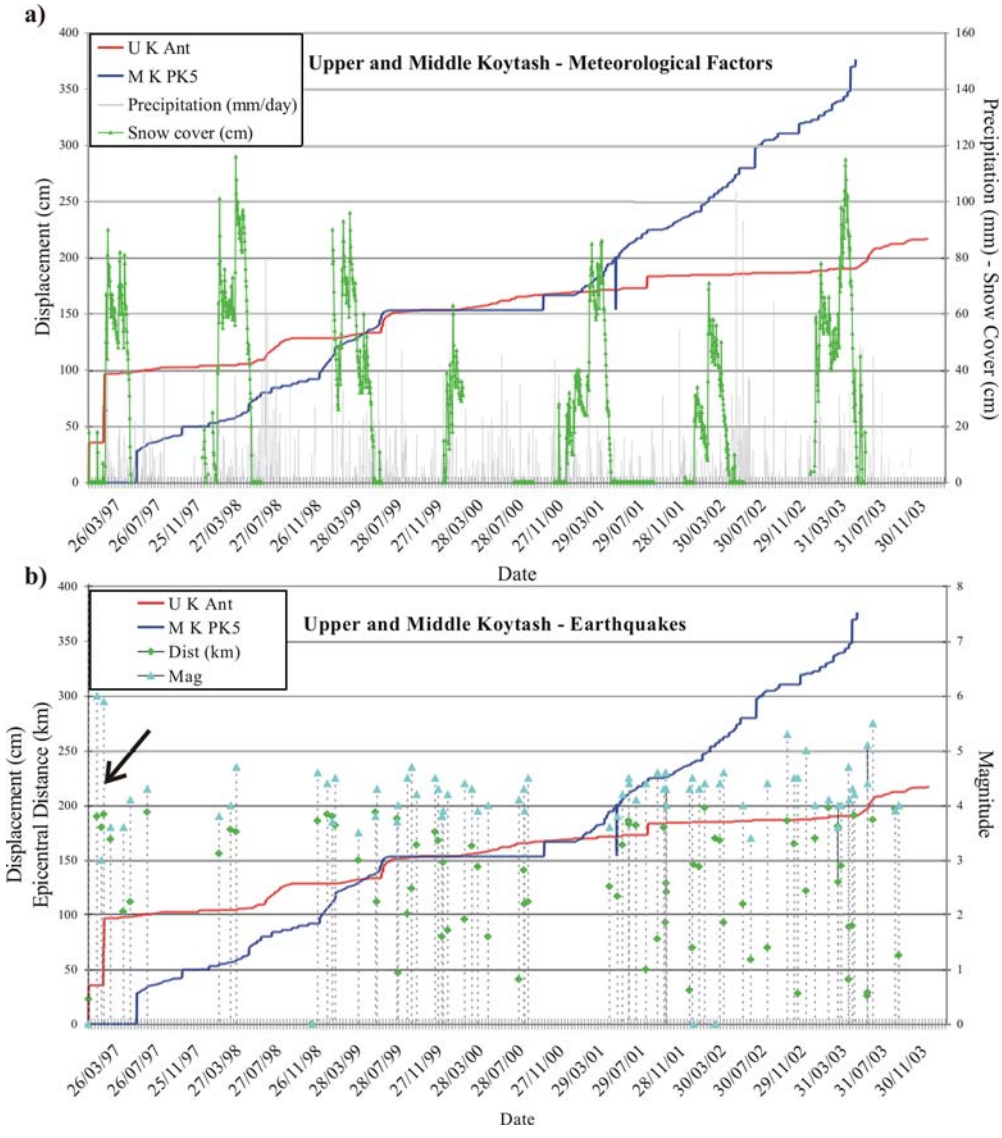

Fig. 7 Extensometer displacement measurements (cm) at the Antenna on Upper Koytash (*dark grey curve*) and point 5 in Middle Koytash (PK5, *light grey curve*) correlated with meteorological factors (**a**, see legend) and local seismicity (b, see legend) with indication of one possible seismic activation (*black arrow*)

Table 1 Summary of results obtained for ten LS analyses

Combination[a]	Max Sc	Counts	PP[b]
S	1.7	102189	1.9
S-A	3.2	896	2.6
S-C	2.0	24	2.0
C-A	6.1	34	1.8
S-A-C	24.4	1	3.0
PC123	27.7	2	3.1
PC123-S-A	27.7	1	12.5
PC12-S-A-C	27.7	1	19.1
G-S-A-C	15.5	1	10.6
F-G-S-A-C	15.5	1	31.6

The respective results obtained for scarp and landslide body location are similar and will only be shown for the first ones; hence, the susceptibility of a UCU is here defined as the map-scaled density of UCU within scarps (Sc).

(a) Combination: S-SLOPE, A-ASPECT, C-CURVATURE, G-GEOLOGY, F-FAULT DISTANCE, PCxyz-Principal Components x,y,z (the first five combinations were carried out over the ASTER image mosaic, the three following, over the northern ASTER image, and the two last over the GEOLOGY map.
(b) Predictive power values.

LS mapping based on a single factor (here the SLOPE angle) is characterized by a low PP (Table 1). Comparison of results obtained for the three pair-combinations involving morphological factors reveals that CURVATURE has the least influence on landslide distribution. The predictive power of the map combining all three morphological factors is 3, similar to that of the map produced by the combination of the three first principal component images. In order to take into consideration both the morphological and spectral information, principal component images were combined with the two important morphological factors, SLOPE and ASPECT (a combination with the third factor was not possible due to computational limits). This allowed us to construct a susceptibility map with a predictive power of up to 12.5 on the basis of the northern ASTER image alone. The combination

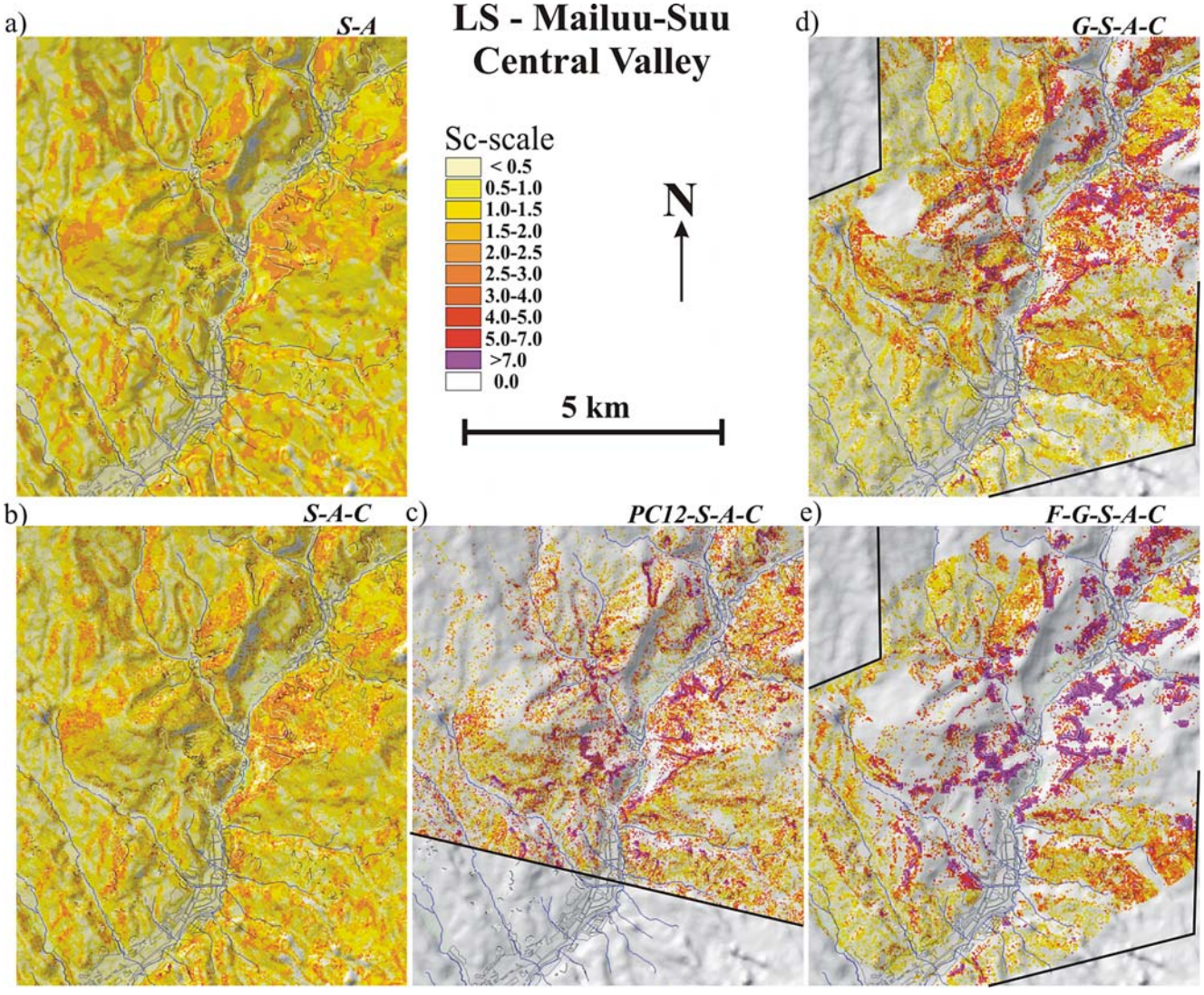

Fig. 8 Comparison between five different LS maps of the Mailuu-Suu Valley in terms of map-scaled scarp densities (see Sc-scale), overlay of scarps (thin, *black*), landslide bodies (thin, *white*), rivers (*blue*) and town (*grey*). Abbreviations used in the map titles, see below Table 1. Limits of map extents are marked by *black lines*. For performance of the maps see Table 1

of all three morphological factors with two first principal component images results even in a larger predictive power (up to 19); the combination with GEOLOGY produces a predictive power of more than 10. If the FAULT DISTANCE map is added to the latter combination (within the GEOLOGY map extent) the predictive power rises to 31.6. These results indicate the strong influence of geology and tectonics on LS (greater than the effect of morphological factors).

The LS maps (in terms of map-scaled scarp density) corresponding to five different combinations, S-A, S-A-C, G-S-A-C, F-G-S-A-C and PC12-S-A-C (Fig. 8) show that increasing combination complexity allows us to distinguish more clearly high-susceptibility from low-susceptibility zones. Combinations with more than four factors detect highest susceptibilities mainly within existing scarp areas (see Figs. 8c, e). Medium to large susceptibilities can also be found in other areas, showing that there is significant potential to develop new landslides.

A large instability potential was found in a zone west of the Mailuu-Suu region. This zone is now recognized as landslide Bedresai (Fig. 9) mapped only recently, after completion of our analysis. Within the landslide polygon (white) map-scaled landslide density values (using PC12-S-A-C combination) are higher than outside the area of slope instability. This landslide probably occurred in 1993 (but it is difficult to detect it on remote imagery). From this it can be inferred that the method does not predict this landslide occurrence but detects it as existing instability (in addition to other slope failures included in the conditional analysis). Such a "blind detection" confirms the reliability of the method. Its ability to predict future slope failure locations can only be proved by comparing it with future landslide occurrences.

Damming and flooding risk

In the past, landslides have often blocked the main Mailuu-Suu River and some of its tributaries. The likelihood of a future landslide dam can partly be evaluated from the previously shown velocity data. As proposed by Swanson et al. (1986) and Clerici and Perego (2000) damming requires a relatively fast landslide. Koytash and Isolith landslides move with mean annual velocities of 0.6 and 1.5 m, respectively. On the basis of these average values, neither Koytash nor Isolith are likely to block Mailuu-Suu River; only a catastrophic change in its

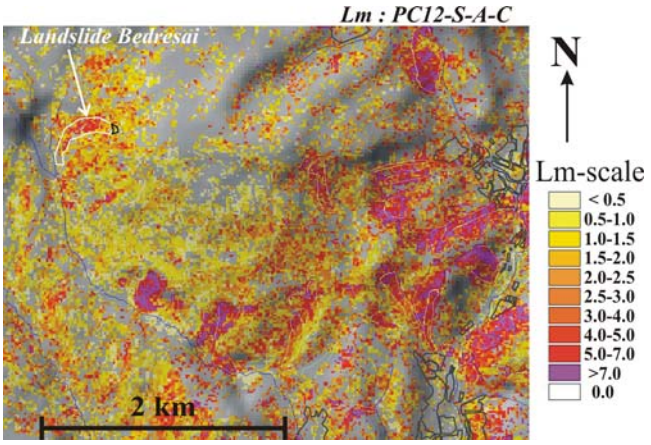

Fig. 9 LS (PC12-S-A-C combination) of the western part of the Mailuu-Suu Valley in terms of map-scaled landslide mass densities (see Lm-scale), overlay of landslide bodies (thin, *white*), and inhabited areas (*dark gray* outlines). The recently mapped landslide Bedresai has been added to compare with LS prediction. For performance of the map see Table 1

activity could result in a dam with significant upstream flooding, such as was observed several times at landslide Tektonik.

In general, the rivers flood during spring to early summer when snowmelt combines with heavy rain. Then, the discharge of the river may reach 100 m^3/s. A particular factor that may add to the discharge of Mailuu-Suu River and enhance the flood risk is a possible outbreak of the mountain lake Kutman Kul, in the headwaters of Mailuu-Suu River at an altitude of 2,841 m (45 km upstream from the town of Mailuu-Suu). This lake formed when the valley was dammed by an ancient rockslide. It has a volume of about 4.5×10^6 m^3. At present, it seems that the likelihood of an outbreak is low, principally because there is no sign of previous overtopping, and the dam crest is more than 5 m higher than the lake level. Water discharge is through the rockslide body. Downstream, the water is collected by another lake, also dammed by rockfalls. This dam is much smaller and regularly overtopped during high river flows.

Preliminary results of GIS-based flooding analyses show that a general rise of Mailuu-Suu River of about 5 m produced by a landslide-dam breach in the headwaters would affect only tailings close to the river channel (e.g., tailing no. 7 immediately upstream of landslide Koytash, see Fig. 3a). The same would also be partially inundated by flooding upstream of a 10–15 m high dam formed by landslide Koytash located several tens of meters downstream of tailing no. 7. However, as discussed above, Koytash seems to move too slowly to overcome river erosion processes affecting the landslide foot. Flooding upstream of a dam formed by landslide Tektonik is a more acute problem because movement of this landslide can, especially at the end of spring, quickly turn from creeping to collapsing. In the future, upstream flooding will probably have little effect on the tailings, but will affect buildings and other constructions. The possible affects of downstream flooding on tailings (notable tailing no. 3) and people have still to be evaluated.

Discussion

A major issue highlighted by analysis of the evolution of recent landslides is the continual increase in the number of slope failures and area of unstable slopes. Is this trend likely to continue?

The potential for future slope instability is of some importance. Therefore, an analysis of landslide susceptibility has been made. This analysis shows that, in addition to existing landslide sites, there are still large areas of slopes that could become unstable in the future. Hence, there is a potential for the total landslide area to increase and for existing landslides to get bigger. Analysis of previous landslide developments showed that either the area of mass movements will enlarge or large landslides will be formed as smaller slope failures coalesce. Both mechanisms were considered in outlining four possible future large landslides on the landslide susceptibility map (map-scaled landslide-mass density for PC12-S-A-C combination in Fig. 10a and G-S-A-C combination in Fig. 10b): growth of Tektonik landslide (dark blue, $\sim 0.5 \times 10^6$ m^2), coalescing of landslides around landslide Koytash (light blue, $\sim 1.2 \times 10^6$ m^2), and close to Upper Mailuu-Suu (blue, $\sim 0.65 \times 10^6$ m^2); a new large landslide west of Kara Agash (greyish blue, $\sim 0.7 \times 10^6$ m^2) due to the higher landslide susceptibility along the slope close to Kara Agash (only indicated by the G-S-A-C map).

The next step is to evaluate how long it will take to develop such large landslides. If the general trends of number and size of landslides are considered (and assuming that the datasets are reliable), the total area affected by failures could triple by 2100 (10% is now affected, and it could reach 30% by 2100). The area of the largest landslide appears to depend on the total landslide area: a large landslide such as shown on Fig. 10 around Koytash (1.2×10^6 m^2) could form within $\sim$150 years (present area of 3.4×10^5 m^2 formed over $\sim$50 years).

Such predictions assume that the slope stability is stationary over time; however, we think that the future evolution depends on the relative importance of anthropic (past mining and now collapsing galleries) and natural factors (climate and earthquakes). If anthropic factors were (and still are) important, destabilization will possibly cease in the future, and landslide activity will slow. If, however, human activity acted only as a local trigger without long-lasting influence, landslide evolution in recent years can only be explained by the strong climatic influence. In which case, slope destabilization is likely to continue in the future and could accelerate under critical conditions (successive wet seasons, and combinations of wet conditions and seismic ground motions).

This last scenario is likely because a strong climatic influence can be shown to be present in the observations and monitoring, whereas the impact of mining can only be inferred from their spatial and temporal proximity.

Our speculations need to be checked, and when landslide activity becomes stationary, the recurrence of landslide events should be estimated on the basis of size-frequency relationships that include also the time factor. The size-frequency relationships presented above refer only to frequency in size (how much) and not to frequency in time (how often). Therefore, the following estimates of potential socio-economic impacts of landslide activity are deterministic (time-independent) and not probabilistic (probability of event within a certain time interval).

Major impacts of future activations are indicated in Fig. 10 marking possible direct effects on people (and tailings) and indirect effects due to damming (white and black arrows, respectively). Three important tailings could be affected by future slope movements: tailing no. 3 (T3 in Fig. 10b) by collapse of the overhanging portion of Tektonik, tailing no. 6 (T6 in Fig. 10b) by destabilization of neighboring slopes, and tailing no. 8 by a collapse of landslide Isolith (T8 in Fig. 10b). Note that the maps mainly represent the potential for coherent slides and not for debris flows which could develop in many other areas and affect other tailings, e.g., tailing no. 7 (directly in the south of T6), as it happened in 1958.

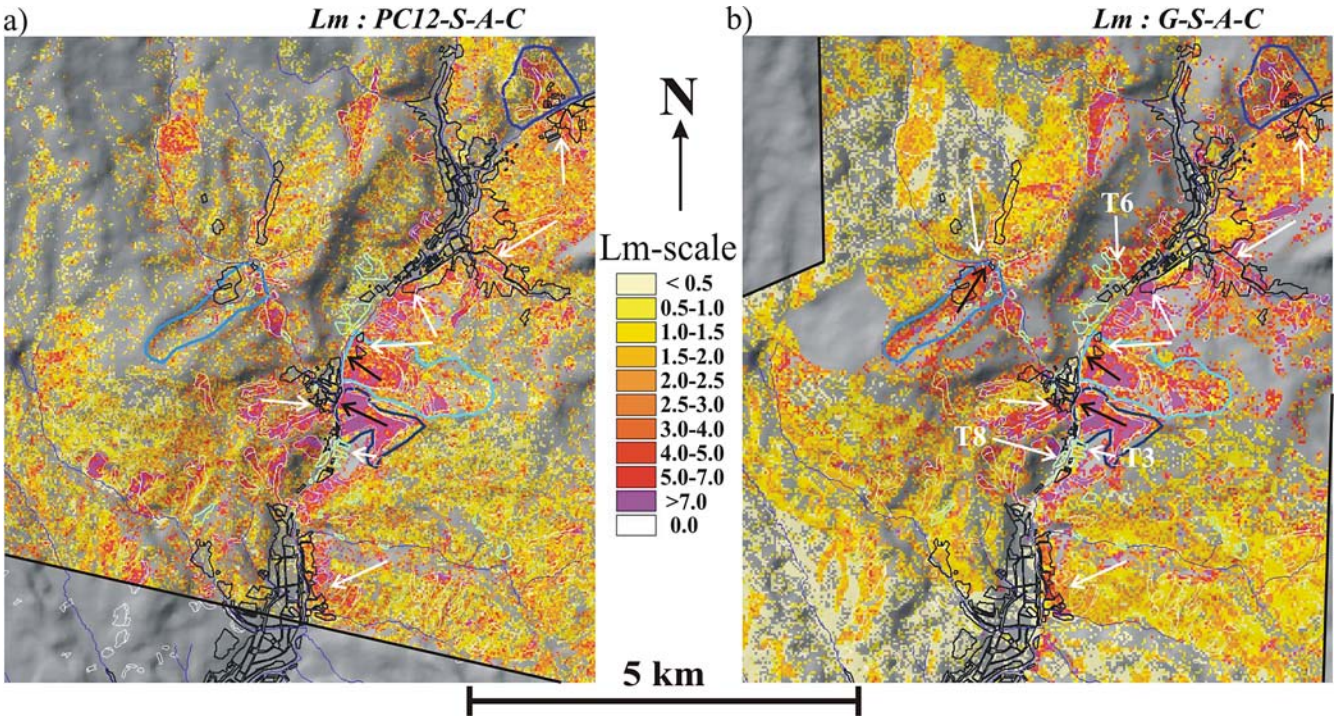

Fig. 10 Two alternative landslide susceptibility maps of the Mailuu-Suu Valley in terms of map-scaled landslide mass densities (see Lm-scale), overlay of landslide bodies (thin, *white*), tailings (*light green*) and inhabited areas (*black outlines*). Possible future large landslides are outlined in *blue*, possible direct impacts on people (and tailings no. 3–T3, no. 6–T6, no. 8–T8) are indicated by *white arrows*, indirect impacts due to damming by *black arrows*

Numerous inhabited areas are located very close to slopes having high landslide susceptibility, such as the northeastern part of the town Mailuu-Suu, the village of Kara Agash at the foot of the northern tongue of Tektonik, and the eastern part of Upper Mailuu-Suu. In addition, some landslides are populated areas themselves (e.g., several houses on landslides Koytash). Also in the future, a large landslide west of Kara Agash could both directly and indirectly affect people, the latter by damming the small river of Kara Agash.

Mitigating the risk in the Mailuu-Suu Valley recently has been recognized as a major priority. Previous and present projects propose many remediation measures, such as a tunnel to by-pass possible future dams formed by Koytash or Tektoink, relocation of tailings (e.g., tailing no. 3 added to tailing no. 6—however, note the high landslide susceptibility close to this latter site). Most of these suggestions evaluate today's situation and do not consider possible future landslides. In particular, a massive landslide of more than 10^7 m^3 would cause many additional problems, which would not be solved by the proposed measures. In the worst case, mitigation may not be "economic" but will require a very large investment. Artificial dams upstream in the central valley, and spill-ways in existing landslide dams are needed to control flooding, and reduce the hazard related to flood waves. If a deep by-pass tunnel along the western riverbank opposite to the Koytash and Tektonik landslides were to be constructed to permanently deviate the waters of Mailuu-Suu River, it should be designed to cope with future large landslide developments. Buttresses are needed in the dry riverbed to support the foot of landslides Koytash and Tektonik. Study is needed of the possibility of reducing the ground water inflow through the Central fault zone. Draining systems are needed in the permeable soils and behind the headscarps of the major landslides to reduce surface-water inflow from the heights. Also, all tailings close to Mailuu-Suu River (no. 3, 5, 6, 7, 8, 9, 18) need to be removed and stored in flat sites beyond the valley bottom.

Conclusions

The present paper discusses landslide-related hazards and associated impacts in the central Mailuu-Suu Valley. A major episode of landslide activation started a few years after the beginning of uranium mining in the 1940s and, hence, is likely to be connected with the mining. Some major landslides have already caused "local-scale" disasters, such as "Tektonik" which has dammed Mailuu-Suu River several times since its major collapse in 1992. Associated upstream and downstream flooding affected numerous buildings and destroyed parts of the factory "Kirghizelektroisolith".

Observations made over the last 50 years and ongoing monitoring have shown that landslide activity is increasing (with constant rate of destabilization). Large landslides tend to develop either by simple growth, or by smaller landslides coalescing. Landslide susceptibility analyses suggest that several large landslides (areas larger than 0.5×10^6 m^2, volumes larger than 8×10^6 m^3) could develop around existing landslides (Koytash and Tektonik, at present, the two largest, with volumes of about 5×10^6 and 3×10^6 m^3, respectively) or at new places, such as west of Kara Agash.

The size of a mass movement is not the only important factor, the dynamics can even be more critical; a slow-moving large landslide such as Koytash does not present a major risk as such. If it accelerates, however, the hazard of a major blockage of Mailuu-Suu River will be significantly increased. An external trigger that is able to strongly accelerate movement is seismic shaking. Thus, it is important to determine the regional seismic hazard of the area as well as local ground-motion effects that may contribute to slope failure.

The landslide danger in this valley is significantly aggravated by the presence of nuclear waste dumps and tailings. These abandoned remnants of the former uranium-mining industry are exposed to erosion, which degrades their protection. Some tailing dams may be directly destroyed by landslide movement, such as the tailings no. 3, 6, and 8. Others could be affected by landslide-dam-induced flooding (e.g., tailing no. 7). Their destabilization could pollute the hydrosphere.

At present, landslide evolution cannot be predicted in terms of probability of occurrence within a certain time period. We are only able to conclude that the threat of landslides, flooding, and related tailing destruction is "hanging" over the town of Mailuu-Suu and the regions downstream like a Damocles sword—it is likely to fall but we do not know when it will fall.

Acknowledgement

The research leading to this article was funded by the NATO Collaborative Linkage Grant for the project *Risk related to earthquakes, landslides and spreading of radioactive waste tailings in Mailuu-Suu (Kyrgyzstan)*. Hans-Balder Havenith thanks the Fonds National de la Recherche Scientifique of Belgium for the 5-years' financial support of his research at the University of Liege, Belgium, on landslide risk in Kyrgyzstan. We also acknowledge Oliver Korup from the Swiss Federal Institute for Forest, Snow and Landscape Research for pre-reviewing and constructive comments on the manuscript.

References

Abdrakhmatov K, Havenith HB, Delvaux D, Jongmans D, Trefois P (2003) Probabilistic PGA and arias intensity maps of Kyrgyzstan (Central Asia). J Seism 7:203–220

Al-Rousan N, Cheng P, Petrie G, Toutin T, Valadan Zoej MJ (1997) Automated DEM extraction and orthoimage Generation from SPOT 1B imagery. Photogram Eng Remote Sens 63(8):965–974

Atkinson PM, Massari R (1998) Generalised linear modelling of susceptibility to landsliding in the Central Apennines, Italy. Compute Geosci 24(4):373–385

Ayalew L, Yamagashi H, Ugawa N (2004) Landslide susceptibility mapping using GIS-based weighted linear combination, the case in Tsugawa area of Agano River, Niigata Prefecture, Japan. Landslides 1:73–81

Carrara A, Cardinali M, Guzzetti F, Reichenbach P (1995) GIS technology in mapping landslide hazard. In: Carrara A, Guzzetti F (eds) Geographical information systems in assessing natural hazards. Kluwer, Dordrecht, pp 135–175

Clerici A, Perego S (2000) Simulation of the Parma River blockage by the Corniglio landside (Northern Italy). Geomorphology 33:1–23

Clerici A, Perego S, Tellini C, Vescovi P (2002) A procedure for landslide susceptibility zonation by the conditional analysis method. Geomorphology 48:349–364

Ercanoglu M, Gokceoglu C (2002) Assessment of landslide susceptibility for landslide-prone area (north of Yenice, NW Turkey) by fuzzy approach. Environ Geol 41:720–730

Fernández-Steeger TM (2002) Erkennung von Hangrutschungssystemen mit Neuralen Netzen als Grundlage für Georisikoanalysen. PhD Thesis, Universität Karlsruhe

Gritzner ML, Marcus WA, Aspinall R, Custer SG (2001) Assessing landslide potential using GIS, soil wetness modeling and topographic attributes, Payette River, Idaho. Geomorphology 37:149–165

Guzzetti F, Carrara A, Cardinali M, Reichenbach P (1999) Landslide hazard evaluation: a review of current techniques and their application in a multi-scale study, Central Italy. Geomorphology 31:181–216

Havenith HB, Strom A, Cacerez F, Pirard E (in press) Analysis of landslide susceptibility in the Suusamyr region, Tien Shan: statistical and geotechnical approach. Landslides

Khazai B, Sitar N (2000) Assessment of seismic slope stability using GIS modeling. Geog Inform Sci 6(2):121–128

Lee S, Ryu JH, Won JS, Park HJ (2004) Determination and application of the weights for landslide susceptibility mapping using an artificial neural network. Eng Geol 71:289–302

Malamud BD, Turcotte DL, Guzzetti F, Reichenbach P (2004) Landslide inventories and their statistical properties. Earth Surf Process Landf 29:687–711

Roessner S, Wetzel HU, Kaufmann H, Sarnagoev A (2002) Satellite remote sensing for regional assessment of landslide in Kyrgyzstan (Central Asia). In: Forum Katastrophenvorsorge, Deutsches Komitee für Katastrophenvorsorge e.V. (DKKV), pp 433–441

Stark CP, Hovius N (2001) The characterization of landslide size distributions. Geophys Res Lett 28:1091–1094

Swanson FJ, Oyagi N, Tominaga M (1986) Landslide dams in Japan. In: Landslide dams: processes, risk and mitigation. Schuster RL (ed) Am Soc Eng Geotech Spec Publ 3, pp 131–145

Torgoev IA, Alioshin YG, Havenith HB (2002) Impact of uranium mining and processing on the environment of mountainous areas of Kyrgyzstan. In: Merkel, Planer-Friedrich and Wolkersdorfer (eds) Uranium in the aquatic environment. Springer, Berlin Heidelberg New York, pp 93–98

Vanacker V, Vanderschaeghe M, Govers G, Willems E, Poesen J, Deckers J, De Bievre B (2003) Linking hydrological, infinite slope stability and land-use change models through GIS for assessing the impact of deforestation on slope stability in high Andean watersheds. Geomorphology 52:299–315

Vandenhove H, Quarch H, Clerc J, Lejeune J, Sweeck L, Sillen X, Mallants D, Zeevaert T (2003) Remediation of uranium mining and milling tailing in Mailuu-Suu district of Kyrgyzstan. Tacis Project N° SCRE1/N°38 Report

H. B. Havenith (✉)
Swiss Seismological Service, Institute of Geophysics,
ETH-Hönggerberg,
8093 Zürich, Switzerland
e-mail: havenith@sed.ethz.ch
Tel.: +41-044-6333380
Fax: +41-044-6331065

I. Torgoev · Y. Alioshin · A. Torgoev
Scientific Engineering Center "GEOPRIBOR",
98 Mederova St.,
720035 Bishkek, Kyrgyz Republic

A. Meleshko
Ministry of the Ecology and Emergency of Kyrgyz Republic,
2/1 Toktonalieva St., Bishkek, Kyrgyz Republic

G. Danneels
Département GeomaC, University of Liege,
B52/3, Sart Tilman B52,
4000 Liège, Belgium